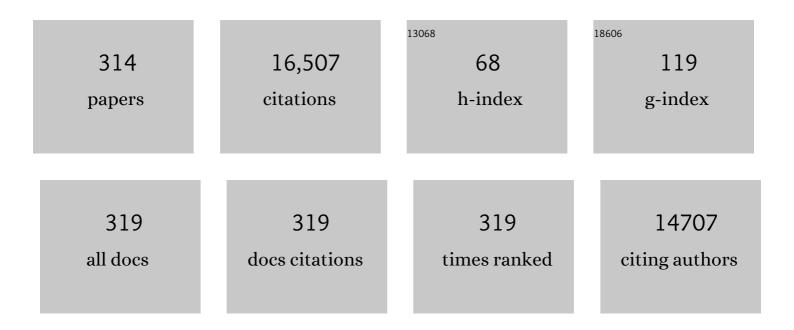
## L Jay Guo

## List of Publications by Year in descending order

Source: https://exaly.com/author-pdf/2561011/publications.pdf Version: 2024-02-01



#	Article	IF	CITATIONS
1	Plasmonic nanoresonators for high-resolution colour filtering and spectral imaging. Nature Communications, 2010, 1, 59.	5.8	687
2	Recent progress in nanoimprint technology and its applications. Journal Physics D: Applied Physics, 2004, 37, R123-R141.	1.3	657
3	Highâ€Speed Rollâ€toâ€Roll Nanoimprint Lithography on Flexible Plastic Substrates. Advanced Materials, 2008, 20, 2044-2049.	11.1	571
4	Large-Area Roll-to-Roll and Roll-to-Plate Nanoimprint Lithography: A Step toward High-Throughput Application of Continuous Nanoimprinting. ACS Nano, 2009, 3, 2304-2310.	7.3	571
5	Organic Solar Cells Using Nanoimprinted Transparent Metal Electrodes. Advanced Materials, 2008, 20, 4408-4413.	11.1	492
6	Biochemical sensors based on polymer microrings with sharp asymmetrical resonance. Applied Physics Letters, 2003, 83, 1527-1529.	1.5	455
7	Efficiency Enhancement of Organic Solar Cells Using Transparent Plasmonic Ag Nanowire Electrodes. Advanced Materials, 2010, 22, 4378-4383.	11.1	343
8	High Performance Bianisotropic Metasurfaces: Asymmetric Transmission of Light. Physical Review Letters, 2014, 113, 023902.	2.9	317
9	Nanofluidic diodes. Chemical Society Reviews, 2010, 39, 923-938.	18.7	297
10	Fabrication of Size-Controllable Nanofluidic Channels by Nanoimprinting and Its Application for DNA Stretching. Nano Letters, 2004, 4, 69-73.	4.5	286
11	Nanoscale Protein Patterning by Imprint Lithography. Nano Letters, 2004, 4, 853-857.	4.5	276
12	Transparent Cu nanowire mesh electrode on flexible substrates fabricated by transfer printing and its application in organic solar cells. Solar Energy Materials and Solar Cells, 2010, 94, 1179-1184.	3.0	223
13	An Ultrathin, Smooth, and Low‣oss Alâ€Doped Ag Film and Its Application as a Transparent Electrode in Organic Photovoltaics. Advanced Materials, 2014, 26, 5696-5701.	11.1	221
14	Experiment and Theory of the Broadband Absorption by a Tapered Hyperbolic Metamaterial Array. ACS Photonics, 2014, 1, 618-624.	3.2	208
15	Rectified Ion Transport through Concentration Gradient in Homogeneous Silica Nanochannels. Nano Letters, 2007, 7, 3165-3171.	4.5	205
16	Angle-Insensitive Structural Colours based on Metallic Nanocavities and Coloured Pixels beyond the Diffraction Limit. Scientific Reports, 2013, 3, 1194.	1.6	200
17	Transparent and Flexible Polarization-Independent Microwave Broadband Absorber. ACS Photonics, 2014, 1, 279-284.	3.2	199
18	Carbon-Nanotube Optoacoustic Lens for Focused Ultrasound Generation and High-Precision Targeted Therapy. Scientific Reports, 2012, 2, 989.	1.6	188

#	Article	lF	CITATIONS
19	Ionic Current Rectification, Breakdown, and Switching in Heterogeneous Oxide Nanofluidic Devices. ACS Nano, 2009, 3, 575-584.	7.3	178
20	Highâ€Performance Flexible Transparent Electrode with an Embedded Metal Mesh Fabricated by Costâ€Effective Solution Process. Small, 2016, 12, 3021-3030.	5.2	178
21	High efficiency resonance-based spectrum filters with tunable transmission bandwidth fabricated using nanoimprint lithography. Applied Physics Letters, 2011, 99, .	1.5	175
22	Flexible conjugated polymer photovoltaic cells with controlled heterojunctions fabricated using nanoimprint lithography. Applied Physics Letters, 2007, 90, 123113.	1.5	167
23	Photonic Color Filters Integrated with Organic Solar Cells for Energy Harvesting. ACS Nano, 2011, 5, 7055-7060.	7.3	167
24	Simple hydrothermal synthesis of very-long and thin silver nanowires and their application in high quality transparent electrodes. Journal of Materials Chemistry A, 2016, 4, 11365-11371.	5.2	154
25	Polymer microring resonators fabricated by nanoimprint technique. Journal of Vacuum Science & Technology an Official Journal of the American Vacuum Society B, Microelectronics Processing and Phenomena, 2002, 20, 2862.	1.6	153
26	Boosted ultraviolet electroluminescence of InGaN/AlGaN quantum structures grown on high-index contrast patterned sapphire with silica array. Nano Energy, 2020, 69, 104427.	8.2	150
27	Structural Colors: From Plasmonic to Carbon Nanostructures. Small, 2011, 7, 3128-3136.	5.2	149
28	Carbon nanotube composite optoacoustic transmitters for strong and high frequency ultrasound generation. Applied Physics Letters, 2010, 97, 234104.	1.5	144
29	Ultrasmooth and Thermally Stable Silver-Based Thin Films with Subnanometer Roughness by Aluminum Doping. ACS Nano, 2014, 8, 10343-10351.	7.3	143
30	Engineering Light at the Nanoscale: Structural Color Filters and Broadband Perfect Absorbers. Advanced Optical Materials, 2017, 5, 1700368.	3.6	141
31	A Facile Route to Polymer Solar Cells with Optimum Morphology Readily Applicable to a Rollâ€ŧoâ€Roll Process without Sacrificing High Device Performances. Advanced Materials, 2010, 22, E247-53.	11.1	131
32	Fabrication and characterization of High Q polymer micro-ring resonator and its application as a sensitive ultrasonic detector. Optics Express, 2011, 19, 861.	1.7	128
33	Ultrathin-metal-film-based transparent electrodes with relative transmittance surpassing 100%. Nature Communications, 2020, 11, 3367.	5.8	123
34	Nanoimprint Lithography Based Approach for the Fabrication of Largeâ€Area, Uniformlyâ€Oriented Plasmonic Arrays. Advanced Materials, 2008, 20, 1129-1134.	11.1	121
35	Colored ultrathin hybrid photovoltaics with high quantum efficiency. Light: Science and Applications, 2014, 3, e215-e215.	7.7	112
36	Strong Resonance Effect in a Lossy Mediumâ€Based Optical Cavity for Angle Robust Spectrum Filters. Advanced Materials, 2014, 26, 6324-6328.	11.1	111

#	Article	lF	CITATIONS
37	Bilayer metal wire-grid polarizer fabricated by roll-to-roll nanoimprint lithography on flexible plastic substrate. Journal of Vacuum Science & Technology B, 2007, 25, 2388.	1.3	110
38	Compact Multilayer Film Structures for Ultrabroadband, Omnidirectional, and Efficient Absorption. ACS Photonics, 2016, 3, 590-596.	3.2	108
39	One-step lithography for various size patterns with a hybrid mask-mold. Microelectronic Engineering, 2004, 71, 288-293.	1.1	106
40	Pure optical photoacoustic microscopy. Optics Express, 2011, 19, 9027.	1.7	106
41	Enhanced Light Utilization in Semitransparent Organic Photovoltaics Using an Optical Outcoupling Architecture. Advanced Materials, 2019, 31, e1903173.	11.1	105
42	Optical generation of high frequency ultrasound using two-dimensional gold nanostructure. Applied Physics Letters, 2006, 89, 093901.	1.5	103
43	Highâ€Colorâ€Purity Subtractive Color Filters with a Wide Viewing Angle Based on Plasmonic Perfect Absorbers. Advanced Optical Materials, 2015, 3, 347-352.	3.6	103
44	A combined-nanoimprint-and-photolithography patterning technique. Microelectronic Engineering, 2004, 71, 277-282.	1.1	101
45	High-frequency ultrasound sensors using polymer microring resonators. IEEE Transactions on Ultrasonics, Ferroelectrics, and Frequency Control, 2007, 54, 957-965.	1.7	101
46	Ultrabroad Bandwidth and Highly Sensitive Optical Ultrasonic Detector for Photoacoustic Imaging. ACS Photonics, 2014, 1, 1093-1098.	3.2	100
47	Micron-scale organic thin film transistors with conducting polymer electrodes patterned by polymer inking and stamping. Applied Physics Letters, 2006, 88, 063513.	1.5	94
48	High-sensitivity and wide-directivity ultrasound detection using high Q polymer microring resonators. Applied Physics Letters, 2011, 98, 204103.	1.5	93
49	Continuous and scalable fabrication of flexible metamaterial films via roll-to-roll nanoimprint process for broadband plasmonic infrared filters. Applied Physics Letters, 2012, 101, .	1.5	93
50	Low density carbon nanotube forest as an index-matched and near perfect absorption coating. Applied Physics Letters, 2011, 99, .	1.5	92
51	Highâ€Performance Doped Silver Films: Overcoming Fundamental Material Limits for Nanophotonic Applications. Advanced Materials, 2017, 29, 1605177.	11.1	90
52	Colored, see-through perovskite solar cells employing an optical cavity. Journal of Materials Chemistry C, 2015, 3, 5377-5382.	2.7	89
53	Highly Transparent and Broadband Electromagnetic Interference Shielding Based on Ultrathin Doped Ag and Conducting Oxides Hybrid Film Structures. ACS Applied Materials & Interfaces, 2019, 11, 11782-11791.	4.0	88
54	Broadband all-optical ultrasound transducers. Applied Physics Letters, 2007, 91, .	1.5	87

#	Article	IF	CITATIONS
55	High performance broadband absorber in the visible band by engineered dispersion and geometry of a metal-dielectric-metal stack. Applied Physics Letters, 2012, 101, .	1.5	86
56	Photo–Roll Lithography (PRL) for Continuous and Scalable Patterning with Application in Flexible Electronics. Advanced Materials, 2013, 25, 6554-6561.	11.1	86
57	Efficient real-time detection of terahertz pulse radiation based on photoacoustic conversion by carbon nanotube nanocomposite. Nature Photonics, 2014, 8, 537-542.	15.6	86
58	Choice of electrode geometry for accurate measurement of organic photovoltaic cell performance. Applied Physics Letters, 2008, 92, 133301.	1.5	84
59	Large Area High Density Sub-20 nm SiO <sub>2</sub> Nanostructures Fabricated by Block Copolymer Template for Nanoimprint Lithography. ACS Nano, 2009, 3, 2601-2608.	7.3	83
60	Decorative power generating panels creating angle insensitive transmissive colors. Scientific Reports, 2014, 4, 4192.	1.6	83
61	Optimization of thermally reduced graphene oxide for an efficient hole transport layer in polymer solar cells. Organic Electronics, 2013, 14, 591-598.	1.4	81
62	Polarization rotation with ultra-thin bianisotropic metasurfaces. Optica, 2016, 3, 427.	4.8	74
63	Efficient Photoacoustic Conversion in Optical Nanomaterials and Composites. Advanced Optical Materials, 2018, 6, 1800491.	3.6	74
64	Ultrathin metal-semiconductor-metal resonator for angle invariant visible band transmission filters. Applied Physics Letters, 2014, 104, .	1.5	73
65	Review of Imprinted Polymer Microrings as Ultrasound Detectors: Design, Fabrication, and Characterization. IEEE Sensors Journal, 2015, 15, 3241-3248.	2.4	73
66	Highly efficient and reliable high power LEDs with patterned sapphire substrate and strip-shaped distributed current blocking layer. Applied Surface Science, 2015, 355, 1013-1019.	3.1	72
67	All-optical scanhead for ultrasound and photoacoustic dual-modality imaging. Optics Express, 2012, 20, 1588.	1.7	71
68	Highâ€Performance Ta <sub>2</sub> O <sub>5</sub> /Alâ€Đoped Ag Electrode for Resonant Light Harvesting in Efficient Organic Solar Cells. Advanced Energy Materials, 2015, 5, 1500768.	10.2	71
69	Printed photonic elements: nanoimprinting and beyond. Journal of Materials Chemistry C, 2016, 4, 5133-5153.	2.7	71
70	Ultrasound detection using polymer microring optical resonator. Applied Physics Letters, 2004, 85, 5418-5420.	1.5	68
71	Toward Low-Cost, High-Efficiency, and Scalable Organic Solar Cells with Transparent Metal Electrode and Improved Domain Morphology. IEEE Journal of Selected Topics in Quantum Electronics, 2010, 16, 1807-1820.	1.9	68
72	Wide-angle, polarization-independent ultrathin broadband visible absorbers. Applied Physics Letters, 2016, 108, .	1.5	68

#	Article	IF	CITATIONS
73	Organic Photovoltaic Cells: From Performance Improvement to Manufacturing Processes. Small, 2015, 11, 2228-2246.	5.2	65
74	Highly Efficient Guiding of Microtubule Transport with Imprinted CYTOP Nanotracks. Small, 2005, 1, 409-414.	5.2	64
75	Thinâ€Metalâ€Filmâ€Based Transparent Conductors: Material Preparation, Optical Design, and Device Applications. Advanced Optical Materials, 2021, 9, 2001298.	3.6	64
76	Polymer Microring Resonators for High-Frequency Ultrasound Detection and Imaging. IEEE Journal of Selected Topics in Quantum Electronics, 2008, 14, 191-197.	1.9	60
77	Integrated intravascular ultrasound and photoacoustic imaging scan head. Optics Letters, 2010, 35, 2892.	1.7	60
78	In vivo flow speed measurement of capillaries by photoacoustic correlation spectroscopy. Optics Letters, 2011, 36, 4017.	1.7	58
79	Large-Area High Aspect Ratio Plasmonic Interference Lithography Utilizing a Single High- <i>k</i> Mode. ACS Nano, 2016, 10, 4039-4045.	7.3	58
80	Semitransparent and Flexible Mechanically Reconfigurable Electrically Small Antennas Based on Tortuous Metallic Micromesh. IEEE Transactions on Antennas and Propagation, 2017, 65, 150-158.	3.1	58
81	High-Resolution Functional Epoxysilsesquioxane-Based Patterning Layers for Large-Area Nanoimprinting. ACS Nano, 2010, 4, 4776-4784.	7.3	56
82	Highly stable and stretchable graphene–polymer processed silver nanowires hybrid electrodes for flexible displays. Journal of Materials Chemistry C, 2015, 3, 1528-1536.	2.7	56
83	Neutral- and Multi-Colored Semitransparent Perovskite Solar Cells. Molecules, 2016, 21, 475.	1.7	56
84	Application of patterned sapphire substrate for III-nitride light-emitting diodes. Nanoscale, 2022, 14, 4887-4907.	2.8	56
85	High-resolution organic polymer light-emitting pixels fabricated by imprinting technique. Journal of Vacuum Science & Technology an Official Journal of the American Vacuum Society B, Microelectronics Processing and Phenomena, 2002, 20, 2877.	1.6	55
86	Low-noise wideband ultrasound detection using polymer microring resonators. Applied Physics Letters, 2008, 92, 193509.	1.5	55
87	Photoacoustic correlation spectroscopy and its application to low-speed flow measurement. Optics Letters, 2010, 35, 1200.	1.7	55
88	Nano-structural characteristics of carbon nanotube–polymer composite films for high-amplitude optoacoustic generation. Nanoscale, 2015, 7, 14460-14468.	2.8	55
89	Semitransparent Cu electrode on a flexible substrate and its application in organic light emitting diodes. Journal of Vacuum Science & Technology B, 2007, 25, 2637.	1.3	54
90	A unique resonance mode observed in a prism-coupled micro-tube resonator sensor with superior index sensitivity. Optics Express, 2007, 15, 17424.	1.7	54

#	Article	IF	CITATIONS
91	Effect of Polymer Aggregation on the Open Circuit Voltage in Organic Photovoltaic Cells: Aggregation-Induced Conjugated Polymer Gel and its Application for Preventing Open Circuit Voltage Drop. ACS Applied Materials & Interfaces, 2011, 3, 674-680.	4.0	53
92	Characterization of a broadband all-optical ultrasound transducer-from optical and acoustical properties to imaging. IEEE Transactions on Ultrasonics, Ferroelectrics, and Frequency Control, 2008, 55, 1867-1877.	1.7	52
93	All-optical photoacoustic microscopy. Photoacoustics, 2015, 3, 143-150.	4.4	52
94	Angular- and polarization-independent structural colors based on 1D photonic crystals. Laser and Photonics Reviews, 2015, 9, 354-362.	4.4	51
95	Continuous phase-shift lithography with a roll-type mask and application to transparent conductor fabrication. Nanotechnology, 2012, 23, 344008.	1.3	50
96	Air-coupled ultrasound detection using capillary-based optical ring resonators. Scientific Reports, 2017, 7, 109.	1.6	50
97	Enhancing the Purity of Reflective Structural Colors with Ultrathin Bilayer Media as Effective Ideal Absorbers. Advanced Optical Materials, 2019, 7, 1900739.	3.6	49
98	High-Performance Large-Scale Flexible Optoelectronics Using Ultrathin Silver Films with Tunable Properties. ACS Applied Materials & Interfaces, 2019, 11, 27216-27225.	4.0	47
99	Miniaturized all-optical photoacoustic microscopy based on microelectromechanical systems mirror scanning. Optics Letters, 2012, 37, 4263.	1.7	46
100	Rollâ€ŧoâ€Roll Cohesive, Coated, Flexible, Highâ€Efficiency Polymer Lightâ€Emitting Diodes Utilizing ITOâ€Free Polymer Anodes. Small, 2013, 9, 4036-4044.	5.2	46
101	Laserâ€Induced Focused Ultrasound for Cavitation Treatment: Toward Highâ€Precision Invisible Sonic Scalpel. Small, 2017, 13, 1701555.	5.2	46
102	Ultraviolet imprinting and aligned ink-jet printing for multilayer patterning of electro-optic polymer modulators. Optics Letters, 2013, 38, 1597.	1.7	44
103	A step toward next-generation nanoimprint lithography: extending productivity and applicability. Applied Physics A: Materials Science and Processing, 2015, 121, 343-356.	1.1	44
104	Angle Robust Reflection/Transmission Plasmonic Filters Using Ultrathin Metal Patch Array. Advanced Optical Materials, 2016, 4, 1981-1986.	3.6	44
105	Vivid-colored silicon solar panels with high efficiency and non-iridescent appearance. Nanoscale Horizons, 2019, 4, 874-880.	4.1	44
106	Benchmarking deep learning-based models on nanophotonic inverse design problems. , 2022, 1, 210012-210012.		43
107	Organic thin film transistors and polymer light-emitting diodes patterned by polymer inking and stamping. Journal Physics D: Applied Physics, 2008, 41, 105115.	1.3	42
108	Spontaneous Formation of Periodic Nanostructures by Localized Dynamic Wrinkling. Nano Letters, 2010. 10. 4228-4234.	4.5	40

#	Article	IF	CITATIONS
109	Facile route of flexible wire grid polarizer fabrication by angled-evaporations of aluminum on two sidewalls of an imprinted nanograting. Nanotechnology, 2012, 23, 344018.	1.3	40
110	ITOâ€Free, Compact, Color Liquid Crystal Devices Using Integrated Structural Color Filters and Graphene Electrodes. Advanced Optical Materials, 2014, 2, 435-441.	3.6	40
111	Highly Efficient Photoacoustic Conversion by Facilitated Heat Transfer in Ultrathin Metal Film Sandwiched by Polymer Layers. Advanced Optical Materials, 2017, 5, 1600421.	3.6	40
112	Transparent Perfect Microwave Absorber Employing Asymmetric Resonance Cavity. Advanced Science, 2019, 6, 1901320.	5.6	40
113	<b>Efficient Thermal–Light Interconversions Based on Optical Topological Transition in the Metalâ€Đielectric Multilayered Metamaterials</b> . Advanced Materials, 2016, 28, 3017-3023.	11.1	38
114	Angleâ€Insensitive and CMOS ompatible Subwavelength Color Printing. Advanced Optical Materials, 2016, 4, 1696-1702.	3.6	38
115	Breaking Malus' law: Highly efficient, broadband, and angular robust asymmetric light transmitting metasurface. Laser and Photonics Reviews, 2016, 10, 791-798.	4.4	38
116	Polymer microring resonators for high-sensitivity and wideband photoacoustic imaging. IEEE Transactions on Ultrasonics, Ferroelectrics, and Frequency Control, 2009, 56, 2482-2491.	1.7	37
117	A fiber-optic system for dual-modality photoacoustic microscopy and confocal fluorescence microscopy using miniature components. Photoacoustics, 2013, 1, 30-35.	4.4	37
118	Imprinted Polymer Microrings as High-Performance Ultrasound Detectors in Photoacoustic Imaging. Journal of Lightwave Technology, 2015, 33, 4318-4328.	2.7	37
119	Comparative study of GaN-based ultraviolet LEDs grown on different-sized patterned sapphire substrates with sputtered AIN nucleation layer. Japanese Journal of Applied Physics, 2017, 56, 111001.	0.8	37
120	On-chip, high-sensitivity temperature sensors based on dye-doped solid-state polymer microring lasers. Applied Physics Letters, 2017, 111, .	1.5	37
121	Automated multi-layer optical design via deep reinforcement learning. Machine Learning: Science and Technology, 2021, 2, 025013.	2.4	37
122	Thermal-flow technique for reducing surface roughness and controlling gap size in polymer microring resonators. Applied Physics Letters, 2004, 84, 2479-2481.	1.5	36
123	Micro-ultrasonic cleaving of cell clusters by laser-generated focused ultrasound and its mechanisms. Biomedical Optics Express, 2013, 4, 1442.	1.5	36
124	Printable thermo-optic polymer switches utilizing imprinting and ink-jet printing. Optics Express, 2013, 21, 2110.	1.7	36
125	Metal transfer assisted nanolithography on rigid and flexible substrates. Journal of Vacuum Science & Technology B, 2008, 26, 2421-2425.	1.3	35
126	Transition from a spectrum filter to a polarizer in a metallic nano-slit array. Scientific Reports, 2014, 4, 3614.	1.6	35

#	Article	IF	CITATIONS
127	Inverse design of metasurface optical filters using deep neural network with high degrees of freedom. InformaÄnÃ-Materiály, 2021, 3, 432-442.	8.5	35
128	SPPs coupling induced interference in metal/dielectric multilayer waveguides and its application for plasmonic lithography. Optics Express, 2012, 20, 12521.	1.7	34
129	Low <i>f</i> -number photoacoustic lens for tight ultrasonic focusing and free-field micro-cavitation in water. Applied Physics Letters, 2016, 108, .	1.5	34
130	A Reconfigurable Color Reflector by Selective Phase Change of GeTe in a Multilayer Structure. Advanced Optical Materials, 2019, 7, 1801214.	3.6	34
131	Fast Flexible Transistors with a Nanotrench Structure. Scientific Reports, 2016, 6, 24771.	1.6	33
132	Plasmonic Lithography Utilizing Epsilon Near Zero Hyperbolic Metamaterial. ACS Nano, 2017, 11, 9863-9868.	7.3	33
133	Planar Metasurfaces Enable Highâ€Efficiency Colored Perovskite Solar Cells. Advanced Science, 2018, 5, 1800836.	5.6	33
134	Holographic Sampling Display Based on Metagratings. IScience, 2020, 23, 100773.	1.9	33
135	Nanoimprinted electrodes for micro-fuel cell applications. Journal of Power Sources, 2007, 171, 218-223.	4.0	32
136	All-optical scanhead for ultrasound and photoacoustic imaging—Imaging mode switching by dichroic filtering. Photoacoustics, 2014, 2, 39-46.	4.4	30
137	Subwavelength nanocavity for flexible structural transmissive color generation with a wide viewing angle. Optica, 2016, 3, 1489.	4.8	30
138	Dynamic Nanoinscribing for Continuous and Seamless Metal and Polymer Nanogratings. Nano Letters, 2009, 9, 4392-4397.	4.5	29
139	Continuous Patterning of Nanogratings by Nanochannelâ€Guided Lithography on Liquid Resists. Advanced Materials, 2011, 23, 4444-4448.	11.1	29
140	Plasma etch fabrication of 60:1 aspect ratio silicon nanogratings with 200 nm pitch. Journal of Vacuum Science and Technology B:Nanotechnology and Microelectronics, 2010, 28, C6P70-C6P75.	0.6	28
141	Continuous and high-throughput nanopatterning methodologies based on mechanical deformation. Journal of Materials Chemistry C, 2013, 1, 7681.	2.7	28
142	Optimization of polymer photovoltaic cells with bulk heterojunction layers hundreds of nanometers thick: modifying the morphology and cathode interface. Energy and Environmental Science, 2013, 6, 2203.	15.6	28
143	Advanced Heterojunction Structure of Polymer Photovoltaic Cell Generating High Photocurrent with Internal Quantum Efficiency Approaching 100%. Advanced Energy Materials, 2013, 3, 1135-1142.	10.2	28
144	Visualizing Mie Resonances in Low-Index Dielectric Nanoparticles. Physical Review Letters, 2018, 120, 253902.	2.9	28

#	Article	IF	CITATIONS
145	Top illuminated organic photodetectors with dielectric/metal/dielectric transparent anode. Organic Electronics, 2015, 20, 103-111.	1.4	27
146	Achieving pattern uniformity in plasmonic lithography by spatial frequency selection. Nanophotonics, 2018, 7, 277-286.	2.9	27
147	Nozzle-Free Liquid Microjetting via Homogeneous Bubble Nucleation. Physical Review Applied, 2015, 3, .	1.5	26
148	Low-Temperature Oxide/Metal/Oxide Multilayer Films as Highly Transparent Conductive Electrodes for Optoelectronic Devices. ACS Applied Energy Materials, 2021, 4, 6553-6561.	2.5	26
149	Multilayer pattern transfer for plasmonic color filter applications. Journal of Vacuum Science and Technology B:Nanotechnology and Microelectronics, 2010, 28, C6O60-C6O63.	0.6	25
150	Robust Extraction of Hyperbolic Metamaterial Permittivity Using Total Internal Reflection Ellipsometry. ACS Photonics, 2018, 5, 2234-2242.	3.2	25
151	Decorative near-infrared transmission filters featuring high-efficiency and angular-insensitivity employing 1D photonic crystals. Nano Research, 2019, 12, 543-548.	5.8	25
152	Multi-film roll transferring (MRT) process using highly conductive and solution-processed silver solution for fully solution-processed polymer solar cells. Energy and Environmental Science, 2014, 7, 2764-2770.	15.6	24
153	Printed Nanostructures for Organic Photovoltaic Cells and Solutionâ€Processed Polymer Lightâ€Emitting Diodes. Energy Technology, 2015, 3, 340-350.	1.8	22
154	Visually tolerable tiling (VTT) for making a large-area flexible patterned surface. Materials Horizons, 2015, 2, 86-90.	6.4	22
155	Ultrahigh <i>Q</i> Polymer Microring Resonators for Biosensing Applications. IEEE Photonics Journal, 2019, 11, 1-10.	1.0	22
156	Compact Stereo Waveguide Display Based on a Unidirectional Polarization-Multiplexed Metagrating In-Coupler. ACS Photonics, 2021, 8, 1112-1119.	3.2	22
157	Entrance effect on ion transport in nanochannels. Microfluidics and Nanofluidics, 2010, 9, 1033-1039.	1.0	21
158	Localized microâ€scale disruption of cells using laserâ€generated focused ultrasound. Journal of Biophotonics, 2013, 6, 905-910.	1.1	21
159	High-color-purity, angle-invariant, and bidirectional structural colors based on higher-order resonances. Optics Letters, 2019, 44, 86.	1.7	21
160	Continuous fabrication of scalable 2-dimensional (2D) micro- and nanostructures by sequential 1D mechanical patterning processes. Nanoscale, 2014, 6, 14636-14642.	2.8	20
161	Characterizing cellular morphology by photoacoustic spectrum analysis with an ultra-broadband optical ultrasonic detector. Optics Express, 2016, 24, 19853.	1.7	20
162	Selective Photomechanical Detachment and Retrieval of Divided Sister Cells from Enclosed Microfluidics for Downstream Analyses. ACS Nano, 2017, 11, 4660-4668.	7.3	20

#	Article	IF	CITATIONS
163	Sustainable p-type copper selenide solar material with ultra-large absorption coefficient. Chemical Science, 2018, 9, 5405-5414.	3.7	20
164	Electrodeposition of Large Area, Angle-Insensitive Multilayered Structural Colors. ACS Applied Materials & Interfaces, 2019, 11, 29065-29071.	4.0	19
165	Design of plasmonic near field plate at optical frequency. Applied Physics Letters, 2010, 96, 141107.	1.5	18
166	Low-noise small-size microring ultrasonic detectors for high-resolution photoacoustic imaging. Journal of Biomedical Optics, 2011, 16, 056001.	1.4	18
167	Au nanostructure arrays for plasmonic applications: annealed island films versus nanoimprint lithography. Nanoscale Research Letters, 2015, 10, 99.	3.1	18
168	Easy duplication of stamps using UV-cured fluoro-silsesquioxane for nanoimprint lithography. Journal of Vacuum Science & Technology B, 2008, 26, 2426-2429.	1.3	17
169	Ultrasmall Structure Fabrication <i>via</i> a Facile Size Modification of Nanoimprinted Functional Silsesquioxane Features. ACS Nano, 2011, 5, 923-931.	7.3	17
170	Efficiency and stability enhancement of polymer solar cells using multi-stacks of C60/LiF as cathode buffer layer. Organic Electronics, 2013, 14, 469-474.	1.4	17
171	Colored dual-functional photovoltaic cells. Journal of Optics (United Kingdom), 2016, 18, 064003.	1.0	17
172	Effects of edge inclination angles on whispering-gallery modes in printable wedge microdisk lasers. Optics Express, 2018, 26, 233.	1.7	17
173	Fabrication and testing of freestanding Si nanogratings for UV filtration on space-based particle sensors. Nanotechnology, 2009, 20, 325301.	1.3	16
174	Fabrication and Encapsulation of a Shortâ€Period Wire Grid Polarizer with Improved Viewing Angle by the Angledâ€Evaporation Method. Advanced Optical Materials, 2013, 1, 863-868.	3.6	16
175	Optical Simulation of Periodic Surface Texturing on Ultrathin Amorphous Silicon Solar Cells. IEEE Journal of Photovoltaics, 2014, 4, 1337-1342.	1.5	16
176	Controlled Generation of Single Microbubble at Solid Surfaces by a Nanosecond Pressure Pulse. Physical Review Applied, 2014, 2, .	1.5	16
177	Modulation of the effective density and refractive index of carbon nanotube forests via nanoimprint lithography. Carbon, 2018, 129, 8-14.	5.4	16
178	Demonstration of versatile whispering-gallery micro-lasers for remote refractive index sensing. Optics Express, 2018, 26, 5800.	1.7	16
179	Analysis of the sensing properties of silica microtube resonator sensors. Journal of the Optical Society of America B: Optical Physics, 2009, 26, 471.	0.9	15
180	Vertically coupled photonic molecule laser. Applied Physics Letters, 2012, 100, 041103.	1.5	15

#	Article	IF	CITATIONS
181	Sensitivity enhancement in optical micro-tube resonator sensors via mode coupling. Applied Physics Letters, 2013, 103, 013702.	1.5	15
182	Nanowire Grid Polarizers Integrated into Flexible, Gas Permeable, Biocompatible Materials and Contact Lenses. Advanced Optical Materials, 2013, 1, 343-348.	3.6	15
183	Quasi-vertical tapers for polymer-waveguide-based interboard optical interconnects. Photonics Research, 2015, 3, 317.	3.4	15
184	Period reduction lithography in normal UV range with surface plasmon polaritons interference and hyperbolic metamaterial multilayer structure. Applied Physics Express, 2015, 8, 062004.	1.1	15
185	5-nm LiF as an Efficient Cathode Buffer Layer in Polymer Solar Cells Through Simply Introducing a C60 Interlayer. Nanoscale Research Letters, 2017, 12, 543.	3.1	15
186	Fabrication of high aspect ratio Si nanogratings with smooth sidewalls for a deep UV-blocking particle filter. Journal of Vacuum Science & Technology B, 2007, 25, 2645.	1.3	14
187	Dual-frequency focused ultrasound using optoacoustic and piezoelectric transmitters for single-pulsed free-field cavitation in water. Applied Physics Letters, 2013, 103, .	1.5	14
188	Microcavity-Integrated Colored Semitransparent Hybrid Photovoltaics With Improved Efficiency and Color Purity. IEEE Journal of Photovoltaics, 2015, 5, 1654-1658.	1.5	14
189	High Q Long-Range Surface Plasmon Polariton Modes in Sub-wavelength Metallic Microdisk Cavity. Plasmonics, 2011, 6, 183-188.	1.8	13
190	Out-coupling of Longitudinal Photoacoustic Pulses by Mitigating the Phase Cancellation. Scientific Reports, 2016, 6, 21511.	1.6	12
191	Subwavelength Surface Plasmon Optical Cavity—Scaling, Amplification, and Coherence. IEEE Journal of Selected Topics in Quantum Electronics, 2009, 15, 1521-1528.	1.9	11
192	High-speed roll-to-roll nanoimprint lithography on flexible substrate and mold-separation analysis. Proceedings of SPIE, 2009, , .	0.8	11
193	Optical enhancement effects of plasmonic nanostructures on organic photovoltaic cells. Chinese Chemical Letters, 2015, 26, 419-425.	4.8	11
194	Effect of the charge balance on high-efficiency inverted polymer light-emitting diodes. Organic Electronics, 2017, 49, 123-128.	1.4	11
195	New Strategy to Overcome the Instability That Could Speed up the Commercialization of Perovskite Solar Cells. Advanced Materials Interfaces, 2019, 6, 1900134.	1.9	11
196	Transparent Colored Display Enabled by Flat Glass Waveguide and Nanoimprinted Multilayer Gratings. ACS Photonics, 2020, 7, 1418-1424.	3.2	11
197	Tackling light trapping in organic light-emitting diodes by complete elimination of waveguide modes. Science Advances, 2021, 7, .	4.7	11
198	Templateâ€Free Vibrational Indentation Patterning (VIP) of Micro/Nanometerâ€Scale Grating Structures with Realâ€Time Pitch and Angle Tunability. Advanced Functional Materials, 2013, 23, 4739-4744.	7.8	10

#	Article	IF	CITATIONS
199	High-Energy Photon Spectroscopy Using All Solution-Processed Heterojunctioned Surface-Modified Perovskite Single Crystals. ACS Applied Materials & Interfaces, 2019, 11, 33399-33408.	4.0	10
200	Photonic crystal microdisk lasers. Applied Physics Letters, 2011, 98, 131109.	1.5	9
201	Funneling light into subwavelength grooves in metal/dielectric multilayer films. Optics Express, 2013, 21, 3595.	1.7	9
202	Improved solar cell performance by adding ultra-thin Alq3 at the cathode interface. Organic Electronics, 2014, 15, 2710-2714.	1.4	9
203	Resistivity Scaling Transition in Ultrathin Metal Film at Critical Thickness and Its Implication for the Transparent Conductor Applications. Advanced Electronic Materials, 0, , 2100970.	2.6	9
204	An ultra-fast optical shutter exploiting total light absorption in a phase change material. Proceedings of SPIE, 2017, , .	0.8	8
205	Improving the Radiative Efficiency of InGaN Quantum Dots via an Open Top Cavity. ACS Photonics, 2017, 4, 795-799.	3.2	8
206	Broad-Spectrum Ultrathin-Metal-Based Oxide/Metal/Oxide Transparent Conductive Films for Optoelectronic Devices. ACS Applied Materials & amp; Interfaces, 2021, 13, 58539-58551.	4.0	8
207	Broad-band high-efficiency optoacoustic generation using a novel photonic crystal-metallic structure. , 2011, , .		7
208	Nanoimprinting ultrasmall and high-aspect-ratio structures by using rubber-toughened UV cured epoxy resist. Nanotechnology, 2013, 24, 255302.	1.3	7
209	Origin of Gouy Phase Shift Identified by Laser-Generated Focused Ultrasound. ACS Photonics, 2020, 7, 3236-3245.	3.2	7
210	Bioinspired Toughening Mechanisms in a Multilayer Transparent Conductor Structure. ACS Applied Materials & Interfaces, 2022, 14, 7440-7449.	4.0	7
211	Highâ€₽erformance Transparent Broadband Microwave Absorbers. Advanced Materials Interfaces, 2022, 9, .	1.9	7
212	Metrology and instrumentation challenges with high-rate, roll-to-roll manufacturing of flexible electronic systems. Proceedings of SPIE, 2012, , .	0.8	6
213	Reconfigurable Thermo-Optic Polymer Switch Based True-Time-Delay Network Utilizing Imprinting and Inkjet Printing. , 2014, , .		6
214	Controlled synthesis of brightly fluorescent CH <sub>3</sub> NH <sub>3</sub> PbBr <sub>3</sub> perovskite nanocrystals employing Pb(C <sub>17</sub> H <sub>33</sub> COO) <sub>2</sub> as the sole lead source. RSC Advances, 2018, 8, 1132-1139.	1.7	6
215	Atomistic Insights into Aluminum Doping Effect on Surface Roughness of Deposited Ultra-Thin Silver Films. Nanomaterials, 2021, 11, 158.	1.9	6
216	Super-resolution photolithography using dielectric photonic crystal. Optics Letters, 2019, 44, 1182.	1.7	6

#	Article	IF	CITATIONS
217	Integrating Structural Colors with Additive Manufacturing Using Atomic Layer Deposition. ACS Applied Materials & Interfaces, 2022, 14, 31099-31108.	4.0	6
218	Photoacoustic endoscopy using polymer microring resonators. Proceedings of SPIE, 2011, , .	0.8	5
219	Insight of limitations of effective media theory for metal–dielectric multilayer metamaterials. Optics Communications, 2013, 305, 8-12.	1.0	5
220	Achieving angle-insensitive spectrum filter with the slit nanoresonator array structure. Journal of Nanophotonics, 2014, 9, 093795.	0.4	5
221	Enhancing the Efficiencies of Organic Photovoltaic and Organic Light-Emitting Diode Devices by Regular Nano-Wrinkle Patterns. Journal of Shanghai Jiaotong University (Science), 2018, 23, 45-51.	0.5	5
222	Polymer Ring Resonator with a Partially Tapered Waveguide for Biomedical Sensing: Computational Study. Sensors, 2021, 21, 5017.	2.1	5
223	NEUTRON: Neural particle swarm optimization for material-aware inverse design of structural color. IScience, 2022, 25, 104339.	1.9	5
224	Photoacoustic concave transmitter for generating high frequency focused ultrasound. Proceedings of SPIE, 2010, 7564, 75642M.	0.8	4
225	Design and fabrication of an integrated intravascular ultrasound/photoacoustic scan head. , 2010, , .		4
226	Free-Standing Silicon Nanogratings for Extreme UV Rejection. ACS Photonics, 2014, 1, 554-559.	3.2	4
227	Investigation of Printingâ€Based Graded Bulkâ€Heterojunction Organic Solar Cells. Energy Technology, 2015, 3, 414-422.	1.8	4
228	Feasibility Analysis of Nanostructured Planar Focusing Collectors for Concentrating Solar Power Applications. ACS Applied Energy Materials, 2018, 1, 6927-6935.	2.5	4
229	Surface-Emitting Surface Plasmon Polariton Laser in a Second-Order Distributed Feedback Defect Cavity. ACS Photonics, 2019, 6, 612-619.	3.2	4
230	Size-Selective Sub-micrometer-Particle Confinement Utilizing Ionic Entropy-Directed Trapping in Inscribed Nanovoid Patterns. ACS Nano, 2021, 15, 14185-14192.	7.3	4
231	Analysis of surface plasmon guided sub-wavelength microdisk cavity. , 2008, , .		3
232	Detection and quantification of lipid membrane binding on silica micro-tube resonator sensor. , 2008, , .		3
233	All-optical transducer for ultrasound and photoacoustic imaging by dichroic filtering. , 2012, , .		3
234	3D high resolution photoacoustic imaging based on pure optical photoacoustic microscopy with microring resonator. Proceedings of SPIE, 2014, , .	0.8	3

#	Article	IF	CITATIONS
235	Fabrication of contact lens containing high-performance wire grid polarizer. Polymer International, 2017, 66, 1269-1274.	1.6	3
236	Scalable Solution-processed Fabrication Strategy for High-performance, Flexible, Transparent Electrodes with Embedded Metal Mesh. Journal of Visualized Experiments, 2017, , .	0.2	3
237	Plasmonic roller lithography. Nanotechnology, 2019, 30, 105202.	1.3	3
238	High Efficiency Semi-Transparent Organic Photovoltaics. , 2019, , .		3
239	Polarization-controlled efficient and unidirectional surface plasmon polariton excitation enabled by metagratings in a generalized Kretschmann configuration. Optics Express, 2021, 29, 3659.	1.7	3
240	23â€4: Ultrathin Foldable Organic Lightâ€Emitting Diodes with High Efficiency. Digest of Technical Papers SID International Symposium, 2021, 52, 289-292.	0.1	3
241	A new interferometric sensor with ring-feedback MZI. , 0, , .		2
242	Biochemical sensors based on polymer microring resonators. , 2004, , .		2
243	Polymer microring resonators and their sensor applications. , 2008, , .		2
244	Characterization of optical microring ultrasound detector by using a high frequency focused photoacoustic transmitter. Applied Physics Letters, 2009, 95, 144105.	1.5	2
245	Roll-to-Roll Nanoimprinting Metamaterials. Materials Research Society Symposia Proceedings, 2012, 1412, 26.	0.1	2
246	Transition from a color filter to a polarizer of a metallic nano-slit array. , 2013, , .		2
247	Angle-insensitive reflective color filters using lossy materials. , 2013, , .		2
248	Efficient Real-time Detection of Terahertz Pulse Radiation by "Listening to―Photoacoustic Generation. , 2014, , .		2
249	High optical coupling efficiency quasi-vertical taper for polymer waveguide devices. Proceedings of SPIE, 2015, , .	0.8	2
250	Waveguide Grating Color Reflector Using Germanium Telluride. , 2019, , .		2
251	Printed Large-area Flat Optical Component: Metasurfaces for Cylindrical Vector Beam Generation. , 2017, , .		2
252	Conjugated Polymer-Based Flexible Photovoltaic Cells with Controlled Nanostructures. Materials Research Society Symposia Proceedings, 2006, 974, 1.	0.1	1

#	Article	IF	CITATIONS
253	Nanoimprint technology and its applications. , 2007, , .		1
254	Evaluation of optoacoustic conversion efficiency of light-absorbing films for optoacoustic transmitter applications. , 2011, , .		1
255	Enhanced efficiency of organic solar cells with silver nanowire electrodes. Proceedings of SPIE, 2011,	0.8	1
256	All-optical generation and detection of acoustic waves for intravascular ultrasound and photoacoustic imaging. , 2011, , .		1
257	Towards high-rate fabrication of photonic devices utilizing a combination of roll-to-roll compatible imprint lithography and ink jet printing methods. , 2013, , .		1
258	High-performance broadband plasmonic absorber in visible fabricated by nanoimprint lithography. Proceedings of SPIE, 2013, , .	0.8	1
259	Ultra-broad Bandwidth Ultrasound Detector Using Imprinted Polymer Microring Resonator. , 2014, , .		1
260	Air-backed optoacoustic transmitter for high amplitude quasi-monopolar wave. , 2014, , .		1
261	Ultra-thin intrinsic amorphous silicon/organic hybrid structure for decorative photovoltaic applications. , 2014, , .		1
262	Towards roll-to-roll manufacturing of polymer photonic devices. Proceedings of SPIE, 2014, , .	0.8	1
263	Microcavity-Integrated Colored Perovskite Solar Cells. , 2015, , .		1
264	Transparent and mechanically reconfigurable small antenna based on stretchable micromesh. , 2015, , .		1
265	Nanoimprint Lithography: Angle-Insensitive and CMOS-Compatible Subwavelength Color Printing (Advanced Optical Materials 11/2016). Advanced Optical Materials, 2016, 4, 1695-1695.	3.6	1
266	RF beam transmission of x-band PAA system utilizing large-area, polymer-based true-time-delay module developed using imprinting and inkjet printing. , 2016, , .		1
267	Fast flexible thin-film transistors with deep submicron channel enabled by nanoimprint lithography. , 2016, , .		1
268	Photoacoustic spectrum analysis for microstructure characterization using ultra-broad bandwidth optical ultrasonic detector. , 2016, , .		1
269	Performance analyses of plasmonic lithography. Proceedings of SPIE, 2017, , .	0.8	1
270	Pâ€185: Flexible Organic Lightâ€Emitting Diodes with Improved Outcoupling Efficiency. Digest of Technical Papers SID International Symposium, 2020, 51, 2071-2074.	0.1	1

#	Article	IF	CITATIONS
271	Transparent and Flexible Self-Dual Antennas for Hybrid Inductive/Capacitive and Radiative Power Transfer. , 2021, , .		1
272	Label-Free Biochemical Sensors Based on Optical Microresonators. Integrated Analytical Systems, 2009, , 177-227.	0.4	1
273	Enhanced light outcoupling from OLEDs by suppressing guided modes formation using an ultrathin flexible transparent conductor. , 2020, , .		1
274	Printable EO-Polymer Modulators. , 2013, , .		1
275	21â€2: <i>Invited Paper:</i> Improve OLED Light Outcoupling Efficiency by Eliminating Waveguide Mode using Ultrathin Metal Electrode. Digest of Technical Papers SID International Symposium, 2022, 53, 231-234.	0.1	1
276	Polymer microring biochemical sensors using Fano-type resonances. , 0, , .		0
277	Active biosensors with dyed-doped microcavities. , 0, , .		0
278	Ellipsometrically probed plasmonic resonances in a square array of Au nanocubes. , 2007, , .		0
279	Prism-Coupled Silica Micro-tube Resonator as a Bio-sensor. , 2007, , .		0
280	Polymer microring resonator for sensitive and broadband ultrasound detection. , 2008, , .		0
281	RECENT DEVELOPMENT AND APPLICATIONS OF NANOIMPRINT TECHNOLOGY. Annual Review of Nano Research, 2009, , 317-350.	0.2	0
282	Design and characterization of acoustic 4f imaging system by using an optical microring ultrasound detector. Proceedings of SPIE, 2010, 7564, 75642N.	0.8	0
283	Nanostructured metal-insulator-metal resonators for high-resolution color filtering and spectral imaging. Proceedings of SPIE, 2011, , .	0.8	Ο
284	One dimensional photonic crystal microdisk laser. , 2011, , .		0
285	3D high-resolution pure optical photoacoustic microscopy. Proceedings of SPIE, 2012, , .	0.8	Ο
286	Polymer microring resonators for high sensitivity, broadband, wide-directivity ultrasound detection and high-resolution imaging. Proceedings of SPIE, 2012, , .	0.8	0
287	All-optical photoacoustic microscopy using a MEMS scanning mirror. Proceedings of SPIE, 2013, , .	0.8	0

#	Article	IF	CITATIONS
289	Phase-Shift Lithography. , 2014, , 1-10.		Ο
290	Prototype study on a miniaturized dual-modality imaging system for photoacoustic microscopy and confocal fluorescence microscopy. , 2014, , .		0
291	Ultrathin transmission visible spectrum filters with wide viewing angle. , 2014, , .		0
292	54.1: <i>Invited Paper</i> : Structural Colors for Display and Eâ€paper Applications. Digest of Technical Papers SID International Symposium, 2014, 45, 781-784.	0.1	0
293	Micro-bubbles generated by a single focused optoacoustic wave. , 2014, , .		0
294	Nonlinear Magnetic Scattering from Polymer Microring Resonators. , 2015, , .		0
295	Transparent and stretchable chipless RFID fabricated using silver nanowire and 3D printed mask. , 2015, , .		0
296	Advanced Manufacturing Technology of Polymer Photovoltaic Cells. Topics in Applied Physics, 2015, , 349-373.	0.4	0
297	Development of CNT-PDMS optoacoustic transmitters by using a localized photothermal curing process. , 2016, , .		0
298	Light Coupling Engineering of a Double-Pinhole Nanoresonator. Journal of Nanoscience and Nanotechnology, 2016, 16, 8130-8134.	0.9	0
299	Contactless ultrasound detection using an optical ring resonator. Proceedings of SPIE, 2016, , .	0.8	0
300	Half-mode hexagonal substrate integrated waveguide (HMHSIW) structure and its application. , 2017, , .		0
301	Notice of Removal: Laser-generated focused ultrasound for micro-cavitation and its application to high-precision cavitation treatment. , 2017, , .		0
302	Terahertz Pulse Detection Techniques and Imaging Applications. , 0, , .		0
303	Subwavelength nanocavity for flexible structural transmissive color generation with wide viewing angle: publisher's note. Optica, 2017, 4, 345.	4.8	0
304	Editorial: Window Electrodes for Emerging Thin Film Photovoltaics. Frontiers in Materials, 2020, 7, .	1.2	0
305	Demonstration of the one-step continuous fabrication of flexible polymer ridge waveguides via nanochannel-guided lithography. Journal of Industrial and Engineering Chemistry, 2021, 95, 286-291.	2.9	0
306	Pâ€102: Flexible Transparent Organic Lightâ€Emitting Diodes with Suppressed Waveguide Modes. Digest of Technical Papers SID International Symposium, 2021, 52, 1462-1465.	0.1	0

#	Article	IF	CITATIONS
307	High-Performance Flexible Microwave Antennas with Ultra-high Visible Transparency. , 2021, , .		0
308	Dual-function ultra-thin a-Si solar cells for color generation and power harvesting. , 2013, , .		0
309	Polymeric Thermo-Optic Switch with Imprinting and Print-on-Demand Technology. , 2013, , .		Ο
310	10.1063/1.4836315.1., 2013,,.		0
311	Low-Cost Fabrication of Organic Photovoltaics and Polymer LEDs. Green Energy and Technology, 2014, , 227-265.	0.4	Ο
312	High-efficiency, Large-area and Color-stable Flexible Organic Light-emitting Diodes using an Ultra-thin Metal Electrode. , 2017, , .		0
313	Ultrasound detection and imaging using Microring Resonators and Laser Generated Focused Ultrasound. , 2018, , .		0
314	Solution-Processed Angle-Insensitive Structural Colors via Electrodeposition of Thin-Films. , 2019, , .		0